Correlated Rigidity Percolation and Colloidal Gels

Shang Zhang, Leyou Zhang, Mehdi Bouzid, D. Zeb Rocklin, Emanuela Del Gado, and Xiaoming Mao

Phys. Rev. Lett. **123**, 058001 — Published 30 July 2019

DOI: 10.1103/PhysRevLett.123.058001

Correlated rigidity percolation and colloidal gels

Shang Zhang,[1] Leyou Zhang,[1] Mehdi Bouzid,[2,3] D. Zeb Rocklin,[1,4] Emanuela Del Gado,[2] and Xiaoming Mao[1]

[1]*Department of Physics, University of Michigan, Ann Arbor, MI 48109, USA*
[2]*Department of Physics, Institute for Soft Matter Synthesis and Metrology, Georgetown University, Washington, D.C. 20057, USA*
[3]*LPTMS, CNRS, Univ. Paris-Sud, Universit Paris-Saclay, 91405 Orsay, France*
[4]*School of Physics, Georgia Institute of Technology, Atlanta, GA 30332, USA*

(Dated: July 3, 2019)

Rigidity percolation (RP) occurs when mechanical stability emerges in disordered networks as constraints or components are added. Here we discuss RP with structural correlations, an effect ignored in classical theories albeit relevant to many liquid-to-amorphous-solid transitions, such as colloidal gelation, which are due to attractive interactions and aggregation. Using a lattice model, we show that structural correlations shift RP to lower volume fractions. Through molecular dynamics simulations, we show that increasing attraction in colloidal gelation increases structural correlation and thus lowers the RP transition, agreeing with experiments. Hence, the emergence of rigidity at colloidal gelation can be understood as a RP transition, but occurs at volume fractions far below values predicted by the classical RP, due to attractive interactions which induce structural correlation.

Introduction – The emergence of mechanical rigidity in soft amorphous solids is central to many material technology developments from 3D printing with soft, biocompatible inks [1] to designing food texture [2, 3], but it is poorly understood and controlled. The main theoretical framework is based on the idea that locally rigid structures, due to mechanical constraints such as chemical bonds or steric repulsion, percolate through the material. Hence the problem translates into the onset of rigidity in a disordered network of springs, an abstraction of the actual solid, whose rigidity percolation (RP) transition has been intensively studied especially in relation with molecular glasses [4–9]. With respect to percolation phenomena controlled by the geometric connectivity [10], the onset of rigidity requires a mechanically stable spanning cluster able to transmit stresses, a problem intrinsically vectorial and long-range [5]. As a result, compared to geometric percolation, RPs display different critical exponents and occur at *higher* volume fractions (e.g., 63% for site RP on a two-dimensional triangular lattice [11] and 36% for site RP on a three-dimensional face-centered-cubic lattice [12]). It is therefore surprising that soft amorphous solids such as colloidal gels—formed in suspensions of colloidal particles with prevalently attractive interactions (due to dispersion or depletion forces)—can be mechanically rigid at low volume fractions, and even as low as a few percent [13–15].

Basic formulations of RP ignore any structural correlation: bonds or sites are randomly removed from a lattice, with no correlation between them, until the structure loses its rigidity. While this approach provided well-tested predictions for glasses [4], the nature of the rigidity transition can significantly depend on how the final structure is assembled [7, 9, 16]. For example, when rigidity emerges as frictionless spheres jam due to compression, a spanning rigid cluster that includes nearly all particles suddenly appears and, with one more contact, the whole system is stressed [17–20]. This scenario differs from basic RP where the spanning rigid cluster is fractal at the transition, although both transitions (jamming and RP) occur near the isostatic point [18, 21–24], where the mean coordination number equals two times the spatial dimensions, $\langle z\rangle = 2d$. The emergence of rigidity in jamming is so different from the classical RP because the self-organization of the structure, accommodating the repulsive interactions among the particles as they are pushed together, dictates the nature of the rigidity transition. It has been recently suggested that the presence of attractive interactions may further change the nature of the rigidity transition at jamming [25], but the emergence of rigidity when the self-organization of the structure is due to aggregation and gelation in a thermodynamic system [15, 26–29] is a much less explored question and remains fundamentally not understood.

Here we propose and demonstrate that spatial correlations can shift the RP to low volume fractions and are therefore crucial to the onset of rigidity in materials like colloidal gels. Using a lattice model in which sites are occupied with local density correlations, we show that the RP threshold shifts to lower volume fraction as correlation strength increases, albeit with the same critical exponents as the classical RP (Fig. 1ab). Our molecular dynamics (MD) simulations of a colloidal-gel model where particles aggregate due to short-range attractions confirm that increasing interaction strength can lead to RP at progressively lower volume fractions by increasing the correlation strength (Fig. 1cd). A simple way to illustrate how structural correlations move the RP to lower volume fractions is that correlations may organize particles into "smart" thin structures that transmit stress. When particles are arranged on a Warren truss which is rigid (Fig. 1a inset), the volume fraction

of this one-dimensional structure on a two-dimensional plane vanishes in the thermodynamic limit. As we show below, spatial correlations originating from short-range attractive interactions naturally prepare particles into such types of structures, giving rise to rigidity at low volume fractions.

For suspensions of attractive colloidal particles, structural correlations are often accessible in experiments and well rationalized via statistical mechanics: fractal aggregation models, cluster theories and density functional theories provide good understanding of structural correlations resulting from short-range attractive interactions [30–32]. While for polymer gels it has been long understood that not all sub-parts of a gel are necessarily rigid [33], for colloidal gels most of existing studies simply assume that all persistent clusters or sub-structures are rigid, in spite of floppy, non-rigid clusters being observed [34]. Hence gelation has been mainly discussed in terms of the geometric percolation of such structures and of the related particle localization [35–41]. Only recent work has started to address specifically the rigidity rather than just the connectivity [34, 42–47]. A clear view of how the interplay between RP and particle localization in the gel structure gives rise to colloidal gelation has been therefore so far lacking. Our findings provide a novel concept and rigorous theoretical framework for understanding the emergence of rigidity in colloidal gels: the rigidity of aggregates comes from the coordinated organization of many interacting particles rather than from the fact that each single cluster is rigid.

Models and Methods – We use two models to investigate the effect of correlation on rigidity. We work in 2D, to be able to use a very efficient method for identifying rigid clusters, the "pebble game" algorithm [5, 48], to obtain the large numerical samples needed to analyze the RP critical behavior. Nevertheless, all arguments (theoretical and phenomenological) extend to 3D. The first model, the *correlated lattice model*, is a modified version of the site-diluted triangular lattice model for RP [11]. Instead of randomly populating lattice sites with a uniform probability, we put particles on a triangular lattice according to the following protocol. At each step, an empty site is randomly chosen, and a particle is put on this site with probability

$$p = (1-c)^{6-N_{nn}} \tag{1}$$

where N_{nn} is the number of its nearest-neighbor sites which are already occupied ($0 \leq N_{nn} \leq 6$) and c is a dimensionless constant controlling the correlation strength ($0 \leq c < 1$). We start with an empty triangular lattice and repeat this process until a target volume fraction ϕ_l is reached (subscript l denotes "lattice"), which relates to the fraction of occupied sites f through $\phi_l \equiv \pi f/(2\sqrt{3})$. We then obtain a spring network where all nearest neighbor pairs, if both exist, are connected. The limit of $c = 0$ corresponds to the classical RP with no structural correlation (all sites occupied with the same probability).

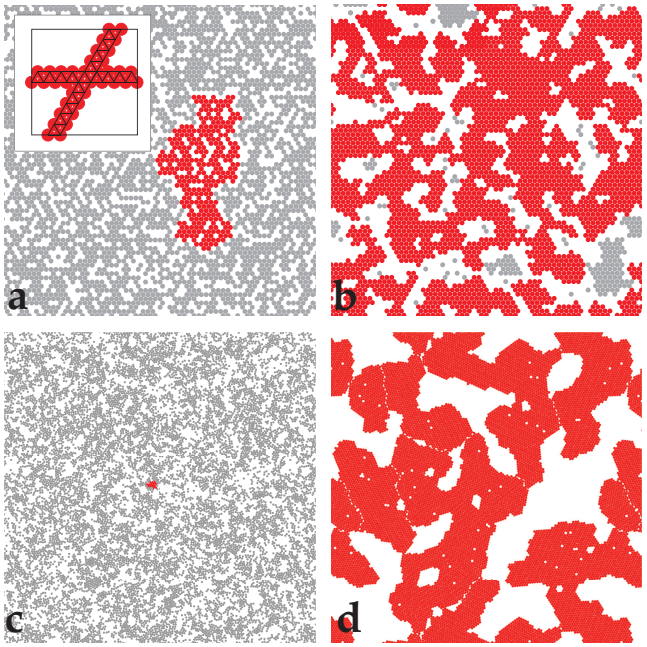

FIG. 1. Examples of rigid cluster decomposition of the correlated lattice model ($\phi_l = 0.6$) at different correlation strengths [$c = 0$ in (a) and $c = 0.6$ in (b)], and the attractive gel model ($\phi_g = 0.6$) at $k_BT/\epsilon = 0.4$ in (c) and 0.1 in (d). Red particles belong to the largest rigid cluster, and other particles are colored in gray. In both models, correlation/attraction induces rigidity at volume fractions below the rigidity transition in the uncorrelated/repulsive limit. The rigid clusters percolate in (b) and (d) where there is strong correlation/attraction, but not in (a) and (c). The inset in (a) shows an extreme example where particles are perfectly correlated (on a Warren truss) and exhibit rigidity at $\phi = 0$ in thermodynamic limit.

The second model, the *attractive gel model*, is an assembly of interacting colloidal particles, studied via molecular dynamics (MD) in 2D. The particles interact through a pairwise Lennard-Jones-like potential which displays a short range attraction (of depth ϵ) and a repulsive core [49, 50]. We generate configurations at different volume fraction ϕ_g (subscript g denotes "gel"), and different ratios between the thermal energy and the attractive well depth k_BT/ϵ, by solving the many-body Newton's equations of motion in a square simulation box with periodic boundary conditions. In spite of its simplicity, our simulations include the essential ingredients of thermodynamics and dynamics in colloidal gels. For each particle configuration, we obtain the corresponding spring network by assigning bonds between pairs of particles of center-to-center distance 1.03σ (the inflection point of the potential) or less. In both models we consider purely central forces, which have been used successfully to understand experiments on colloidal gels in a large part of the literature [15, 41, 43, 49, 51, 52]. Non-central

forces may also be important [53–57] and can be included in our approach through bond-bending rigidity [58–60]. Further details of our simulation protocol are included in the Supplement Information (SI)[61]. We analyze the rigidity of all the spring networks from the two models using the pebble game algorithm [5, 48], which decomposes the networks into rigid clusters. RP occurs when the largest rigid cluster percolates in both directions, leading to macroscopic rigidity [9, 70].

Results – In both models, we find that with correlation/attraction, rigidity emerges at volume fractions lower than in uncorrelated cases (Fig. 1). In the correlated lattice model, we measure two quantities, the probability of having a percolating rigid cluster $P(\phi_l, c, L)$, and the average mass of the largest rigid cluster $\mathcal{M}(\phi_l, c, L)$, where L is the linear size of the lattice. Following the notion of percolation, $\mathcal{M}$ is the order parameter of the transition. As shown in Fig. 2, when the correlation strength c increases, both P and $\mathcal{M}$ curves shift to the left, confirming that RP occurs at a lower ϕ_l in the presence of correlation. Moreover, the gradual increase of $\mathcal{M}$ at the transition suggests that the correlated rigidity transition is still continuous, as the classical RP. The fact that P and $\mathcal{M}$ for different L intersect at the same scale-free point confirms this.

We analyze critical scaling relations near the correlated rigidity transition using finite-size scaling (details in the SI). We first determine the transition point $\phi_{l,c}(c, L)$ where the spanning rigid cluster first appears, averaging over disordered samples. For each c, the transition point shifts as a function of L following standard finite-size scaling relations with correlation length exponent $\nu = 1.21$ (agreeing with classical RP [5]), towards the infinite volume limit, $\phi_{l,c}(c, L = \infty)$. We find that the transition point decreases with c

$$\phi_{l,c}(c = 0, L = \infty) - \phi_{l,c}(c, L = \infty) = a\, c^{1/\zeta}, \quad (2)$$

at small c, where $\zeta \simeq 0.76$, the coefficient $a \simeq 0.19$, and the $c \to 0$ limit transition point is $\phi_{l,c}(0, \infty) \simeq 0.63$ agreeing with the classical RP result (note the extra factor of $\pi/(2\sqrt{3})$ converting from site occupancy probability to volume fraction).

The data for P and $\mathcal{M}$ can then be collapsed using the following scaling forms

$$P(\phi_l, c, L) \sim \tilde{P}[(\phi_l - \phi_{l,c}(c, L = \infty))L^{1/\nu}], \quad (3)$$

$$\mathcal{M}(\phi_l, c, L) \sim L^{d-\beta/\nu}\tilde{\mathcal{M}}[(\phi_l - \phi_{l,c}(c, L = \infty))L^{1/\nu}], \quad (4)$$

where ν and β are the critical exponents for the correlation length and the growth of the order parameter (figures in the SI). These scaling relations share the same form as ones used in classical RP with the same exponents ($\nu = 1.21$ and $\beta = 0.18$) [5], but with correlation dependent transition points $\phi_{l,c}(c, L = \infty)$ which we determine above.

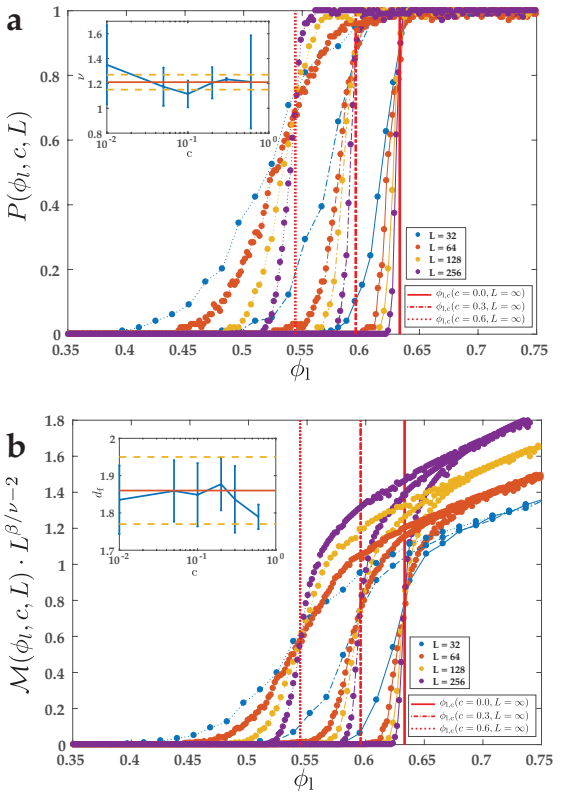

FIG. 2. (a) $P(\phi_l, c, L)$ at different L and c (symbols and line styles defined in legends). Inset: ν for different c (blue with error bars), in comparison with average (red line) and standard error (yellow dashed line) of ν in the classical RP (from Ref. [11]). (b) $\mathcal{M}(\phi_l, c, L)$ at different L and c. Inset: d_f for different c (blue with error bars), in comparison with average (red line) and standard error (yellow dashed line) of ν in the classical RP (from Ref. [11]). In both (a) and (b), curves for different L cross at the same point (marked by red lines), indicating continuous transitions at every c at different $\phi_{l,c}(c, L = \infty)$.

Our results suggest that correlations play the role of an irrelevant perturbation at the RP transition. They shift the transition point $\phi_{l,c}(c, L = \infty)$ while leaving critical exponents the same as in the uncorrelated case. Thus, with correlation, the RP still belongs to the same universality class, as also found in other percolation problems [71, 72]. One way to interpret this result is that the structural correlations we introduce in the model are a short range feature. Although they shift the transition, the critical scaling is controlled largely by the physics at large lengthscales and is not sensitive to microscopic modifications. We confirm this by measuring the critical exponents at different c. In particular, we measure ν via fluctuations of $\phi_{l,c}(c, L)$ over samples, $\Delta_\phi \equiv \sqrt{\langle \phi_{l,c}(c, L)^2 \rangle - \langle \phi_{l,c}(c, L) \rangle^2}$, as well as the fractal dimension of the giant rigid cluster at the transition $\mathcal{M}_c = \langle \mathcal{M}(\phi_{l,c}, c, L) \rangle$. We fit these quantities to their

finite-size scaling relations,

$$\Delta_\phi \sim L^{-1/\nu}, \tag{5}$$

$$\mathcal{M}_c \sim L^{d_f}, \tag{6}$$

where the fractal dimension relates to β by $d_f = d - \beta/\nu$ (here $d = 2$ is the spatial dimension). Within error bars, ν and β agree with those of the classical RP for every c (Fig. 2 insets).

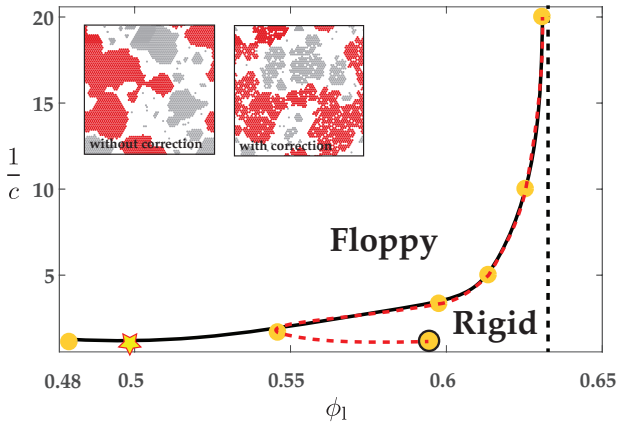

FIG. 3. Phase diagram of the correlated lattice model (without and with the strong correlation correction). Calculated phase boundary $\phi_{l,c}(c, L = \infty)$ are shown as yellow dots (before correction: with black circles around the dots, after correction: without circles; They overlap at small c). The red dashed line and the black solid line show the phase boundaries before and after the correction by connecting the dots, respectively. The $c \to 0$ limit (classical RP) is shown as the black dashed line. The insets are configurations taken at $c = 0.9, \phi_l = 0.5$ (the yellow star) with and without the strong correlation correction, which avoids the formation of disconnected dense blobs and leads to a percolating rigid cluster.

The resulting phase diagram is shown in Fig. 3, with the phase boundary determined from $\phi_{l,c}(c, L = \infty)$. We plot the phase diagram in the ϕ_l vs $1/c$ plane for convenient comparison with the attractive gel model, where we identify the rigid gel states in the ϕ_g vs k_BT/ϵ plane, since correlations decrease as both $1/c$ and k_BT/ϵ increase. In the limit of $1/c \to \infty$ the transition reduces to the classical RP, while the boundary shifts to lower ϕ_l as c increases (as discussed above). However, when c is large (> 0.6) the phase boundary bends back to higher ϕ_l (dashed line in Fig. 3). The reason for this reentrant behavior is that very strong correlations force the particles to aggregate into densely packed blobs that do not percolate. This high c limit would correspond to a separation of the colloid-dense phase in an attractive colloidal suspension, rather than to the colloidal gelation that takes place through dynamical arrest and prevents the formation of disconnected droplets [51, 56, 59]. To better capture gelation, we add a correction for strong correlation: a site can not be occupied if 4 or more of its neighboring sites are already occupied [$p = 0$ when $N_{nn} \geq 4$ and p still obeys Eq. (1) for $N_{nn} < 4$]. With the modified model, the RP transition volume fraction becomes monotonically decreasing as c increases, in better agreement with experiments and our attractive gel simulation described below.

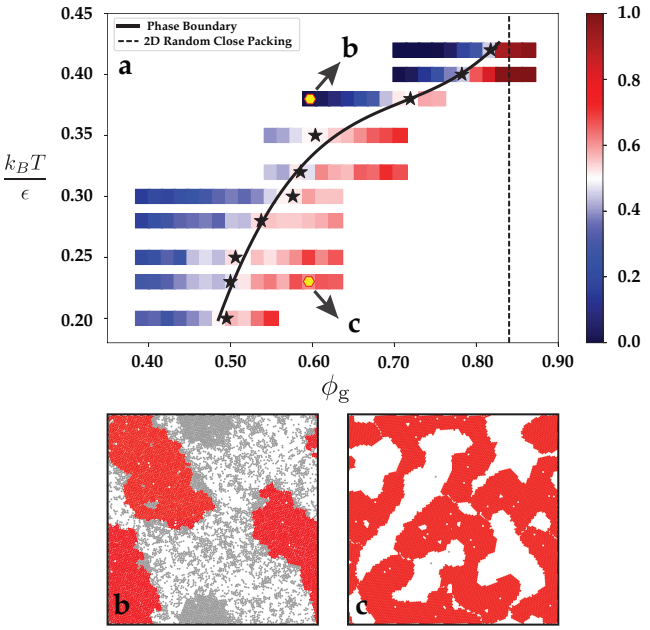

FIG. 4. (a) Phase diagram of the attractive gel model. Simulated parameters $(\phi_g, k_BT/\epsilon)$ are shown as squares colored according to their measured $P_g(\phi_g, k_BT/\epsilon)$ (color scale shown in legend). Black stars show fitted phase boundary at each k_BT/ϵ and the black line is the phase boundary from fitting these transition points to third order polynomial. The hard sphere limit of the transition is shown as a black dashed line. (b,c) show two example configurations with their rigid cluster decomposition, chosen at the two marked points on the phase diagram. The largest rigid cluster percolates in (c) but not in (b), agreeing with the phase boundary.

Results from rigidity analysis of the attractive gel model are shown in Fig. 4. We simulate gels of 10^4 particles in $2D$ at various ϕ_g and k_BT/ϵ, and obtain the mean probability for the emergence of a percolating rigid cluster $P_g(\phi_g, k_BT/\epsilon)$. At each k_BT/ϵ we identify the transition point $\phi_{g,c}(k_BT/\epsilon)$ by fitting $P_g(\phi_g, k_BT/\epsilon)$ as a quadratic function of ϕ_g and find the point where $P_g = 0.5$. These transition points are then fitted to a smooth curve to construct the phase boundary of rigidity in the ϕ_g vs. k_BT/ϵ plane. In Fig. 4ab we show two sample configurations (with rigid cluster decomposition) at the same volume fraction $\phi_g = 0.6$ but for two distinct values $k_BT/\epsilon = 0.23$ and 0.38 . Large thermal fluctuations can frequently break bonds, and the resulting structure is either a homogeneous gas of particles (Fig. 1c) or displays phase separation but the large clusters do not show rigidity percolation yet (as shown in Fig. 4b). In contrast, decreasing k_BT/ϵ, the attraction

is so strong that the particle-rich regions not only percolate through the whole system, but also exhibit rigidity (Fig. 4c). The phase boundary bends down again at very strong attraction, where the system goes out of equilibrium and the rigidity is dominated by the physics of diffusion limited aggregation [73]. The similarity between the phase boundaries in the correlated lattice model and the attractive gel model indicates that the rigidity onset in dilute systems is favored by the structural correlations induced by the attractive interactions. Hence, the emergence of rigidity at colloidal gelation can be understood as a RP transition in which structural correlations help optimize mechanically stable structures [43, 46].

To summarize, we have studied the rigidity transition in a diluted triangular lattice model where particles populate sites with positional correlation, and a colloidal gel model with short range attraction using MD simulation. The two models show similar structural heterogeneities where particles clusters, forming stress-bearing networks that percolate through the system at low volume fractions. We analyze critical scaling exponents in the correlated lattice model, and find that the rigidity transition belongs to the same universality class as the classical RP, but the transition threshold moves to lower volume fractions as correlation increases. The attractive gel model further demonstrates that such structural correlations and heterogeneities can naturally arise as a result of short range attractive interactions in a thermal system. Deeper understandings of how this structural heterogeneity develops in the incipient phase separation and how it depends on the preparation protocol used for the gel (for example, the cooling rate or the gelation kinetics in the simulations) [74], as well as connecting correlated RP scenario obtained here to the hard sphere limit where no attraction is present and rigidity emerges at the random close packing volume fraction (84% in 2D) or to the case in which different types of topological constraints may be present [75], will be intriguing topics to explore in future studies.

We thank M. Solomon for helpful discussions. SZ, LZ, and XM thank the support from the National Science Foundation (Grant No. DMR-1609051). MB and EDG thank the Impact Program of the Georgetown Environmental Initiative and Georgetown University, Kavli Institute for Theoretical Physics at the University of California Santa Barbara and National Science Foundation (Grant No. NSF PHY17-48958).

[1] R. L. Truby and J. A. Lewis, Nature **540**, 371 (2016).
[2] R. Mezzenga, P. Schurtenberger, A. Burbidge, and M. Michel, Nature materials **4**, 729 (2005).
[3] B. Keshavarz, T. Divoux, S. Manneville, and G. H. McKinley, ACS Macro Letters **6**, 663 (2017).
[4] H. He and M. F. Thorpe, Physical Review Letters **54**, 2107 (1985).
[5] D. J. Jacobs and M. F. Thorpe, Physical review letters **75**, 4051 (1995).
[6] M. Sahimi, Physics Reports **306**, 213 (1998).
[7] M. Thorpe, D. Jacobs, M. Chubynsky, and J. Phillips, Journal of Non-Crystalline Solids **266**, 859 (2000).
[8] M. Bauchy and M. Micoulaut, Journal of Non-Crystalline Solids **357**, 2530 (2011).
[9] W. G. Ellenbroek, V. F. Hagh, A. Kumar, M. Thorpe, and M. Van Hecke, Physical review letters **114**, 135501 (2015).
[10] D. Stauffer and A. Aharony, *Introduction to percolation theory: revised second edition* (CRC press, 2014).
[11] D. Jacobs and M. Thorpe, Physical Review E **53**, 3682 (1996).
[12] M. Chubynsky and M. F. Thorpe, Physical Review E **76**, 041135 (2007).
[13] V. Trappe, V. Prasad, L. Cipelletti, P. Segre, and D. Weitz, Nature **411**, 772 (2001).
[14] S. Manley, L. Cipelletti, V. Trappe, A. Bailey, R. Christianson, U. Gasser, V. Prasad, P. Segre, M. Doherty, S. Sankaran, *et al.*, Physical review letters **93**, 108302 (2004).
[15] P. J. Lu, E. Zaccarelli, F. Ciulla, A. B. Schofield, F. Sciortino, and D. A. Weitz, Nature **453**, 499 (2008).
[16] P. Boolchand, D. Georgiev, and B. Goodman, Journal of Optoelectronics and Advanced Materials **3**, 703 (2001).
[17] C. S. O'hern, L. E. Silbert, A. J. Liu, and S. R. Nagel, Physical Review E **68**, 011306 (2003).
[18] A. J. Liu and S. R. Nagel, Annu. Rev. Condens. Matter Phys. **1**, 347 (2010).
[19] C. P. Goodrich, A. J. Liu, and S. R. Nagel, Physical review letters **109**, 095704 (2012).
[20] D. M. Sussman, C. P. Goodrich, and A. J. Liu, Soft matter **12**, 3982 (2016).
[21] X. Mao, N. Xu, and T. C. Lubensky, Phys. Rev. Lett. **104**, 085504 (2010).
[22] W. G. Ellenbroek and X. Mao, Europhys. Lett. **96**, 540002 (2011).
[23] L. Zhang, D. Z. Rocklin, B. G.-g. Chen, and X. Mao, Phys. Rev. E **91**, 032124 (2015).
[24] T. C. Lubensky, C. L. Kane, X. Mao, A. Souslov, and K. Sun, Reports on Progress in Physics **78**, 073901 (2015).
[25] D. J. Koeze and B. P. Tighe, arXiv:1807.06526 [cond-mat.soft] (2018).
[26] V. Trappe, V. Prasad, L. Cipelletti, P. Segre, and D. A. Weitz, Nature **411**, 772 (2001).
[27] G. Lois, J. Blawzdziewicz, and C. S. O'Hern, Physical review letters **100**, 028001 (2008).
[28] D. A. Head, The European Physical Journal E **22**, 151 (2007).
[29] I. Jorjadze, L.-L. Pontani, K. A. Newhall, and J. Brujić, Proceedings of the National Academy of Sciences **108**, 4286 (2011).
[30] T. A. Witten and P. Pincus, *Structured fluids: polymers, colloids, surfactants* (Oxford University Press, 2004).
[31] J.-P. Hansen and I. R. McDonald, *Theory of simple liquids* (Elsevier, 1990).
[32] D. Richard, J. Hallett, T. Speck, and C. P. Royall, Soft matter (2018).
[33] P. G. d. Gennes, *Scaling concepts in polymer physics* (Cornell University Press, Ithaca, N.Y., 1979).
[34] A. Dinsmore and D. Weitz, Journal of Physics: Con-

densed Matter **14**, 7581 (2002).
[35] E. Del Gado, A. Fierro, L. de Arcangelis, and A. Coniglio, Phys. Rev. E **69**, 051103 (2004).
[36] P. N. Segrè, V. Prasad, A. B. Schofield, and D. A. Weitz, Phys. Rev. Lett. **86**, 6042 (2001).
[37] K. Broderix, H. Löwe, P. Müller, and A. Zippelius, Physical Review E **63**, 011510 (2000).
[38] K. Kroy, M. Cates, and W. Poon, Physical review letters **92**, 148302 (2004).
[39] R. Ball, D. Weitz, T. Witten, and F. Leyvraz, Physical review letters **58**, 274 (1987).
[40] M. Lin, H. Lindsay, D. Weitz, R. Ball, R. Klein, and P. Meakin, Nature **339**, 360 (1989).
[41] M. E. Cates, M. Fuchs, K. Kroy, W. C. Poon, and A. M. Puertas, Journal of Physics: Condensed Matter **16**, S4861 (2004).
[42] C. P. Royall, S. R. Williams, T. Ohtsuka, and H. Tanaka, Nature materials **7**, 556 (2008).
[43] N. E. Valadez-Pérez, Y. Liu, A. P. Eberle, N. J. Wagner, and R. Castaneda-Priego, Physical Review E **88**, 060302 (2013).
[44] A. Zaccone, H. Winter, M. Siebenbürger, and M. Ballauff, Journal of Rheology **58**, 1219 (2014).
[45] L. Hsiao, R. S. Newman, S. C. Glotzer, and M. J. Solomon, Proceedings of the National Academy of Sciences **109**, 16029 (2012).
[46] H. Tsurusawa, M. Leocmach, J. Russo, and H. Tanaka, arXiv preprint arXiv:1804.04370 (2018).
[47] D. Z. Rocklin, L. C. Hsiao, M. Szakasits, M. J. Solomon, and X. Mao, manuscript in preparation (2018).
[48] D. J. Jacobs and B. Hendrickson, Journal of Computational Physics **137**, 346 (1997).
[49] V. J. Anderson and H. N. Lekkerkerker, Nature **416**, 811 (2002).
[50] M. Bantawa, M. Bouzid, and E. Del Gado, Manuscript in preparation. (2018).
[51] R. N. Zia, B. J. Landrum, and W. B. Russel, Journal of Rheology **58**, 1121 (2014).
[52] E. D. Gado, D. Fiocco, G. Foffi, S. Manley, V. Trappe, and A. Zaccone, Fluids, Colloids and Soft Materials: An Introduction to Soft Matter Physics , 279 (2016).
[53] V. Prasad, V. Trappe, A. Dinsmore, P. Segre, L. Cipelletti, and D. Weitz, Faraday Discussions **123**, 1 (2003).
[54] A. Dinsmore, V. Prasad, I. Wong, and D. Weitz, Physical review letters **96**, 185502 (2006).
[55] J. P. Pantina and E. M. Furst, Physical review letters **94**, 138301 (2005).
[56] C. J. Dibble, M. Kogan, and M. J. Solomon, Phys. Rev. E **77**, 050401 (2008).
[57] T. Ohtsuka, C. P. Royall, and H. Tanaka, EPL (Europhysics Letters) **84**, 46002 (2008).
[58] C. P. Broedersz, X. Mao, T. C. Lubensky, and F. C. MacKintosh, Nature Physics **7**, 983 (2011).
[59] E. Del Gado and W. Kob, Soft Matter **6**, 1547 (2010).
[60] J. Colombo and E. Del Gado, Soft matter **10**, 4003 (2014).
[61] See Supplemental Material for more details, which includes Refs. [62-69].
[62] G. Laman, Journal of Engineering mathematics **4**, 331 (1970).
[63] J. Machta, Y. Choi, A. Lucke, T. Schweizer, and L. Chayes, Physical Review E **54**, 1332 (1996).
[64] M. E. Newman and R. M. Ziff, Physical Review E **64**, 016706 (2001).
[65] J. Colombo and E. Del Gado, Journal of rheology **58**, 1089 (2014).
[66] D. Frenkel and B. Smit, "Understanding molecular simulation: From algorithms to applications," (2002).
[67] M. G. Noro and D. Frenkel, The Journal of Chemical Physics **113**, 2941 (2000).
[68] S. Plimpton, Journal of computational physics **117**, 1 (1995).
[69] P. J. Steinhardt, D. R. Nelson, and M. Ronchetti, Physical Review B **28**, 784 (1983).
[70] S. Henkes, D. A. Quint, Y. Fily, and J. Schwarz, Physical review letters **116**, 028301 (2016).
[71] A. Coniglio, H. E. Stanley, and W. Klein, Physical Review Letters **42**, 518 (1979).
[72] A. Coniglio, Journal of Physics A: Mathematical and General **12**, 545 (1979).
[73] T. A. Witten and L. M. Sander, Phys. Rev. Lett. **47**, 1400 (1981).
[74] H. Ricateau, L. F. Cugliandolo, and M. Picco, Journal of Statistical Mechanics: Theory and Experiment **2018**, 013201 (2018).
[75] M. Bouzid and E. Del Gado, Langmuir **34**, 773 (2017).